*17th World Conference on Earthquake Engineering, 17WCEE*
*Sendai, Japan - September 13th to 18th 2020*

# Application of Adaptive Time Delay Compensation Combined with Linear-quadratic-gauss in Vehicle-bridge Coupling Real-time Hybrid Simulation

B. Zhang[1], *H. Zhou[2], X. Shao[3], Y. Tian[4], W. Guo[5], T. Wang[6], Q. Gu[7]

[1] *Master student, Institute of engineering mechanics, China Earthquake Administration, 15802974831@163.com*
[*2] *Associated Professor, Institute of engineering mechanics, China Earthquake Administration, zhouhuimeng@iem.ac.cn*
[3] *Associated Professor, Western Michigan University, xiaoyun.shao@wmich.edu*
[4] *Doctoral student, Institute of engineering mechanics, China Earthquake Administration, junfan1234567@163.com*
[5] *Professor, Central South University, guowei@csu.edu.cn*
[6] *Professor, Institute of engineering mechanics, China Earthquake Administration, wangtao@iem.ac.cn*
[7] *Professor, Xiamen University, quangu@xmu.edu.cn*

## *Abstract*

In a recent study to investigate vehicle-rail bridge interaction of high-speed railway system, real-time hybrid simulation (RTHS) is applied to simulate the dynamic response of this coupling system. The railway bridge is selected as the numerical substructure whose dynamic displacement response subject to the moving vehicle's excitation is numerically simulated. The simulated response is then imposed using a uniaxial shaking table onto the high-speed train (i.e., the suspension frame and vehicle body), which is considered as the physical substructure in the RTHS. The measured reaction force of the vehicle is sent back to the bridge model to determine the displacement response of the next time step and forming a closed-loop simulation process. The unique challenge in this RTHS is to compensate the time delay of the high-frequency signals in the vehicle-bridge coupling system. Therefore, an adaptive time series (ATS) compensation algorithm combined with the linear quadratic Gaussian (LQG) is proposed to address this control challenge of RTHS involving high-frequency signals. Different RTHS working conditions, such as different train speed, long-short wave irregularity and varying bridge section stiffness, are tested during which the time-delay compensation's effects are compared between the combined ATS and LQG method (ATS+LQG) and the ATS method only. The root mean square error of commands and responses is used as the evaluating indicator. It was found that the ATS+LQG method outperforms the ATS method in the high frequency range when applied to the RTHS of vehicle-bridge coupling.

*Keywords: RTHS, vehicle-rail bridge coupling system, ATS, ATS+LQG, high-frequency signals*

 



## 1. Introduction

When the train passes the bridge at a relatively high-speed, the factors such as the train speed, the section of the bridge structure, and the level of the track irregularity directly affect the dynamic coupling between the train and the railway girder bridge [1]. To achieve train operation stability, and high level of ride comfort, experimental investigation is necessary to study the vehicle-bridge coupling under different service conditions, during which the interaction between the high-speed train and the bridge needs to accurately reproduced.

The RTHS method, developed based on the pseudo-dynamic test [2], has been adopted in a rapid prototyping railway bogie [3,4]. This simulation method was recently further applied to study the vehicle-bridge coupling problem in which a shaking table was used as the loading equipment. Therefore, when RTHS is applied to the vehicle-bridge coupling system, the challenge to compensate the time-delay involving high-frequency responses of the bridge needs to be addressed. Some scholars proposed adaptive time delay compensation methods for RTHS of building structures [5-6]. For example, Wu et al. [5] proposed an actuator dynamics compensation method based on an upper bound delay, in which the displacement is over-compensated and then the datum that is closest to the desired displacement is selected by an optimal process. Chae et al.[6] proposed to use the second-order Taylor series to calculate the actuators' commands, during which the optimum Taylor series coefficients were determined using the least squares method. However, these adaptive methods were only verified in RTHS of building structures with relatively low frequency responses. To address the time delay compensation challenge in the RTHS of vehicle-bridge coupling with high frequency responses, an adaptive controller combining the adaptive time series compensation with a linear quadratic gaussian [7] was proposed.

The following paper is divided into five sections. The principle of the combined ATS+LQG compensation algorithm is introduced in the second section. The third section is the RTHS experimental design for the vehicle-bridge coupling system which include model substructuring, experimental setup and the working conditions. The experimental verification results are discussed in fourth section. The conclusion summarizes the observations from the verification experiments in fifth section.

## 2. ATS+LQG Compensation Method

Block diagram demonstrating the major components of the proposed ATS+LQG controller is shown in Fig. 1, along with the RTHS setup consisting of the shaking table and the specimen highlighted in red. The ATS+LQG controller includes an LQR controller (shown in green) and a state observer (shown in blue).

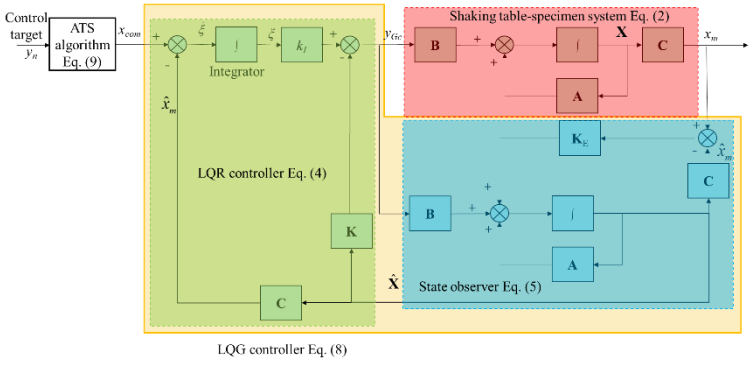


Fig. 1 – Block diagram of the ATS+LQG controller

In Fig. 1, $y_n$ is the output of the numerical substructure. $y_{Gc}$ is the command signal from the controller to the shaking table-specimen system. $x_m$ is the measured displacement of the shaking table and $x_{com}$ is the output of the ATS compensator. The objective of the ATS+LQG controller is to make the measured displacement $x_m$ accurately tracking the output of the numerical substructure $y_n$. To further reduce the time delay effect in the RTHS system, the ATS compensation is integrated that extrapolates the output of the numerical substructure $y_n$ before it is sent to the LQG controller.



 



## 2.1 LQR controller

The design of the LQR controller requires an identified numerical model of the shaking table-specimen system. A linear transfer function model of the system is adopted herein for the convenience of the analysis presented later. This transfer function is expressed as:

$$G_{\mathrm{P}}(s)=\frac{B_0 s^5+B_1 s^4+B_2 s^3+B_3 s^2+B_4 s+B_5}{s^5+A_1 s^4+A_2 s^3+A_3 s^2+A_4 s+A_5} \tag{1}$$

where $B_0$, $B_1$, $B_2$, $B_3$, $B_4$, $B_5$, $A_1$, $A_2$, $A_3$, $A_4$, and $A_5$ are the polinomial coefficients. The state-space model of the shaking table-specimen system is then obtained as:

$$\begin{cases}\dot{\mathbf{X}}=\mathbf{A}\mathbf{X}+\mathbf{B}y_{Gc}\\ x_m=\mathbf{C}\mathbf{X}\end{cases} \tag{2}$$

where $\mathbf{A}=\begin{bmatrix}0&1&0&0&0\\0&0&1&0&0\\0&0&0&1&0\\0&0&0&0&1\\-A_5&-A_4&-A_3&-A_2&-A_1\end{bmatrix}$, $\mathbf{B}=\begin{bmatrix}\beta_1 & \beta_2 & \cdots & \beta_5\end{bmatrix}^T$, and $\mathbf{C}$=[1 0 0 0 0]. $\beta_n$ ($n$=0, 1, …, 5) is determined based on the formula of $\beta_n=B_n-A_1\beta_{n-1}-\cdots-A_n\beta_0$.

To ensure zero steady state error, an integrator is inserted in the feedforward path between the error comparator and the shaking table-specimen to build a type-1 servo system, as shown in Fig. 1 (see the green frame). For the LQR controller, the actuator command is determined as:

$$\begin{cases}y_{Gc}=-\mathbf{K}\mathbf{X}+k_I\xi=-\bar{\mathbf{K}}\bar{\mathbf{X}}\\ \dot{\xi}=x_{com}-x_m=x_{com}-\mathbf{C}\mathbf{X}\end{cases} \tag{3}$$

where $\bar{\mathbf{K}}$=[$\mathbf{K}$ -$k_I$] is the feedback gain matrix of the state $\bar{\mathbf{X}}$ of type-1 servo system, and $\bar{\mathbf{X}}$=$\begin{bmatrix}\mathbf{X} & \xi\end{bmatrix}^T$ is a scalar representing the output of the integrator (i.e., a state variable of the system). Substituting Eq. (3) into Eq. (2), the state-space model of the equivalent regulation problem system becomes:

$$\begin{cases}\dot{\bar{\mathbf{X}}}=\bar{\mathbf{A}}\bar{\mathbf{X}}+\begin{bmatrix}\mathbf{0} & 1\end{bmatrix}^T x_{com}\\ x_m=\bar{\mathbf{C}}\bar{\mathbf{X}}\end{cases} \tag{4}$$

where $\bar{\mathbf{A}}=\begin{bmatrix}\mathbf{A}-\mathbf{B}\mathbf{K} & \mathbf{B}k_I\\ -\mathbf{C} & 0\end{bmatrix}$, and $\bar{\mathbf{C}}=\begin{bmatrix}\mathbf{C} & 0\end{bmatrix}$.

## 2.2 State observer

When the observability condition is satisfied, the state observers can be designed. As shown in Fig. 1, the state observer estimates the state variables based on the measured displacement of the shaking table $x_m$ and the command signal from the controller to the shaking table-specimen system $y_{Gc}$. Thus, the mathematical model of the observer is defined as:

$$\begin{aligned}\dot{\hat{\mathbf{X}}}&=\mathbf{A}\hat{\mathbf{X}}+\mathbf{B}y_{Gc}+\mathbf{K}_{\mathrm{E}}(x_m-\mathbf{C}\hat{\mathbf{X}})=(\mathbf{A}-\mathbf{K}_{\mathrm{E}}\mathbf{C})\hat{\mathbf{X}}+\mathbf{B}y_{Gc}+\mathbf{K}_{\mathrm{E}}x_m\\ \dot{\xi}&=x_{com}-\hat{x}_m=x_{com}-\mathbf{C}\hat{\mathbf{X}}\end{aligned} \tag{5}$$

where $\mathbf{K}_{\mathrm{E}}$ is the observer gain matrix. It is a weighting matrix to the correction term involving the difference between the measured displacement of the shaking table $x_m$ and the estimated displacement of the shaking table $\hat{x}_m=\mathbf{C}\hat{\mathbf{X}}$. This is a full state observer. The observer gain matrix $\mathbf{K}_{\mathrm{E}}$ can be estimated using the *lqe*2 function in the MATLAB Toolbox with the inputs shown below:



 



$$\mathbf{K}_{\mathrm{E}} = lqe2(\mathbf{A}, \mathbf{B}, \mathbf{C}, Q_e, R_e) \tag{6}$$

where $Q_e$ is the covariance matrix of the system noises, and $R_e$ is the covariance matrix of the measurement noises. The LQG controller model may now be expressed as:

$$y_{Gc} = -\mathbf{K}\hat{\mathbf{X}} + k_I \xi \tag{7}$$

Combining Eqs. (5) and (7) leads to:

$$\begin{cases} \dot{\tilde{\mathbf{X}}} = \tilde{\mathbf{A}}\tilde{\mathbf{X}} + \begin{bmatrix} \mathbf{0} & 1 \end{bmatrix}^T x_{com} + \tilde{\mathbf{K}}_{\mathrm{E}} x_m \\ y_{Gc} = -\bar{\mathbf{K}}\tilde{\mathbf{X}} \end{cases} \tag{8}$$

where $\tilde{\mathbf{A}} = \begin{bmatrix} \mathbf{A} - \mathbf{K}_{\mathrm{E}}\mathbf{C} - \mathbf{B}\mathbf{K} & k_I\mathbf{B} \\ -\mathbf{C} & 0 \end{bmatrix}$, $\tilde{\mathbf{K}}_{\mathrm{E}} = \begin{bmatrix} \mathbf{K}_{\mathrm{E}} & 0 \end{bmatrix}^T$, $\tilde{\mathbf{X}}$ is the assemble of the estimate of the state vector $\hat{\mathbf{X}}$ and an intermediate variable $\xi$, expressed as $[\,\hat{\mathbf{X}} \quad \xi\,]^T$.

### 2.3 Adaptive time series (ATS) compensator [6]

The compensated shaking table displacement input is calculated based on the ATS method as:

$$x_{comk} = a_{0k} x_k^c + a_{1k} \dot{x}_k^c + a_{2k} \ddot{x}_k^c \tag{9}$$

where $k$ is the sampling time step number, the sampling time step was set to be 1/1024 sec in the RTHS. The corresponding coefficients can be calculated by equation (10) which is using a matrix/vector as:

$$\mathbf{a} = \left(\mathbf{X}_m^T \mathbf{X}_m\right)^{-1} \mathbf{X}_m^T \mathbf{U}^c \tag{10}$$

in which

$$\mathbf{X}_m = \begin{bmatrix} x_{mk-1} & \dot{x}_{mk-1} & \ddot{x}_{mk-1} \\ x_{mk-2} & \dot{x}_{mk-2} & \ddot{x}_{mk-2} \\ \vdots & \vdots & \vdots \\ x_{mk-q} & \dot{x}_{mk-q} & \ddot{x}_{mk-q} \end{bmatrix}, \mathbf{a} = \begin{bmatrix} a_{0k} \\ a_{1k} \\ a_{2k} \end{bmatrix}, \text{ and } \mathbf{U}^c = \begin{bmatrix} x_{comk-1} \\ x_{comk-2} \\ \vdots \\ x_{comk-q} \end{bmatrix} \tag{11}$$

With the values for the coefficients $a_{jk}$ identified, the compensated actuator displacement input at time $t_k$ is calculated using Eq. (9).The identified two coefficients in Eq. (9) are related to the amplitude error and the time delay as shown below:

$$A_{ek} \cong \frac{1}{a_{0k}}, \tau_k \cong \frac{a_{1k}}{a_{0k}} \tag{12}$$

where $A_{ek}$ and $\tau_k$ are the amplitude error and time delay at the $k^{th}$ step, respectively. When the amplitude error is not significant (i.e., $A_{ek} \cong 1$), $a_{1k}$ is approximately equal to $\tau_k$.

## 3. RTHS Experimental Design

### 3.1 Model substructuring

In the RTHS of the vehicle-bridge coupling system, the numerical substructure (i.e., a high-speed railway bridge) was modeled as a 7-span simply-supported beam of 32 m long (see Fig. 2). The bridge girder has a box-shaped cross section, and the circular bridge piers are 8m high.

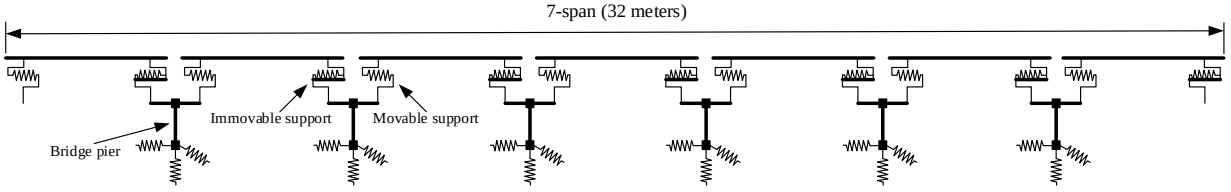


Fig. 2 – Model of numerical substructure



 



A quarter of the CRH380A high-speed rail car locomotive (i.e., one vehicle and two bogies) was selected as the experimental substructure as shown in Fig. 3(a) and its simplified two-degree-of-freedom numerical model is shown in Fig. 3(a), where *Mc*, *Mt* and *Mw* are the mass of the car body, the bogie, and the wheel, respectively. *Ks*, *Kp* and *Cs*, *Cp* are the stiffness and damping coefficients connecting the three masses as shown in the Fig. 3 (b). The values of these parameters are listed in Table 1.

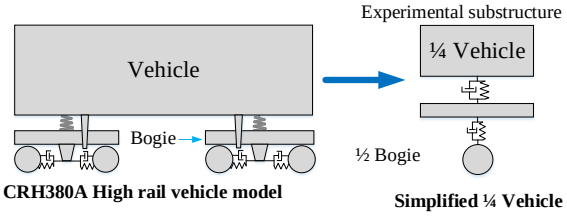


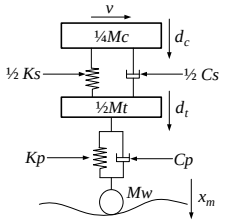


(a) Simplified schematic (b) Simplified model[8]

Fig. 3 – Model of experimental substructure

The dynamic equation of the experimental substructure (i.e., the vehicle) when subject to the road irregularity and bridge deformation was established as:

$$\begin{bmatrix} Mt & 0 \\ 0 & Mc \end{bmatrix}\begin{bmatrix} \ddot{d}_t \\ \ddot{d}_c \end{bmatrix}+\begin{bmatrix} Cp+Cs & -Cs \\ -Cs & Cs \end{bmatrix}\begin{bmatrix} \dot{d}_t \\ \dot{d}_c \end{bmatrix}+\begin{bmatrix} Kp+Ks & -Ks \\ -Ks & Ks \end{bmatrix}\begin{bmatrix} d_t \\ d_c \end{bmatrix}=\begin{bmatrix} Kpx_m+Cp\dot{x}_m \\ 0 \end{bmatrix} \tag{13}$$

where $d_t$, $d_c$ are the motions of the car body and the bogie. The interaction force between the vehicle and the bridge is calculated based on the acceleration response of the vehicle (i.e., the experimental substructure) as:

$$F_{wheel-rail}=Mc\ddot{d}_c+Mt\ddot{d}_t+(Mc+Mt+Mw)\cdot g \tag{14}$$

where, $g$ is the acceleration of gravity. This force is then sent to the bridge model (see Fig. 2) to compute the bridge deformation $y_n$ as the displacement command of the shaking table of each time step.

Table 1 – The equivalent parameters of the simplified model

| | **1/4Vehicle** | **Values** |
|---|---|---|
| **Vehicle** | 1/4*Mc* (kg) | 8446.5 |
| | 1/2*Ks* (N/m) | 225000 |
| | 1/2*Cs* (N*s/m) | 10000 |
| **bogie** | *Mt* (kg) | 1028 |
| | *Kp* (N/m) | 1772000 |
| | *Cp* (N*s/m) | 20000 |
| **Wheelset** | *Mw* (kg) | 1267 |

## 3.2 Experimental setup

During RTHS, the experimental substructure fixed on the shaking table was subject to the shaking table displacement $x_m$. The acceleration responses $\ddot{d}_t$ and $\ddot{d}_c$ of the experimental substructure was the used to compute the interaction force $F_{wheel-rail}$ and sent to the numerical substructure (bridge) so its deformation was solved and became the displacement command $y_n$ to the shaking table. In reality, the interaction force and the displacement responses of the vehicle-bridge coupling system are in the vertical direction. However, a horizontal unidirectional shaking table was utilized as the loading equipment so the experimental substructure was recumbent. The displacement and interaction force in the vertical direction were therefore converted into the horizontal direction, and the gravity of the experimental substructure (i.e., $(Mc+Mt+Mw).g$) was neglected in computing the interaction force in Eq. (14). The car body was installed on a low friction guide rail that was fixed on the bogie, and the bogie was also installed on a low friction guide rail that was fixed on shaking table. The stiffness of the vehicle was provided by springs attached to both ends of the experimental substructure



 



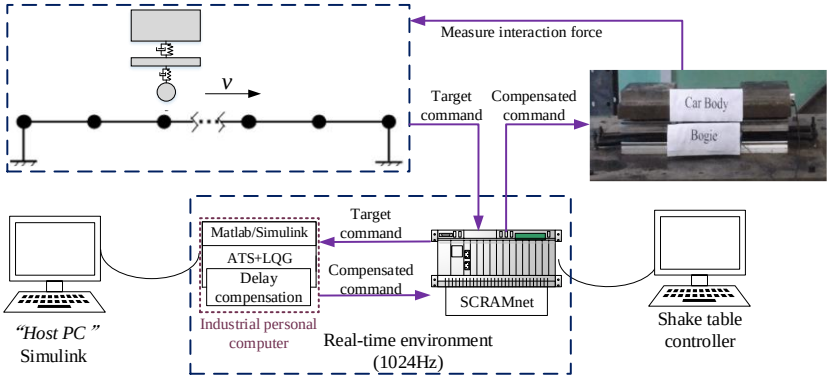


Fig. 4 – Hardware and software diagram of vehicle-bridge coupling system in RTHS

The hardware and software comoponents of the RTHS testing system consist of computers used for numerical simulations (i.e., Host PC, Industrial perponal computer) and a computer used to control the shaking table as shown in Fig. 4. The two real-time computers in the dashed line box are equipped with SCRAMNet and connected with optical fiber to ensure a real-time environment during RTHS. The time step of the RTHS was 1/1024 sec and the shaking table has a time delay of approximately 40 ms. The software adopted in the RTHS testing system are MATLAB/Simulink and its associated xPC-target, which are used to setup up the numerical model and the ATS+LQG compensation, solve the dynamic equation to determine the command displacement and compute the interaction force. The pulsar controller software is utilized to control the shaking table.

### 3.3 RTHS test cases

The box shaped bridge section is shown in Fig. 5 and the parameters of the three bridge cross sections considered tested are listed in Table 2. A total of 8 RTHS test cases that are divided into three groups representing different controlling parameters were tested (see Table 3). Please note that cases 2, 4, and 6 have the same working conditions and they are included in different groups for easy comparison.

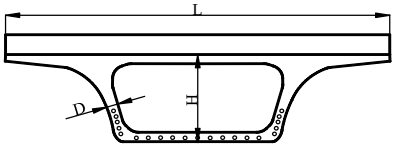


Fig. 5 – Bridge section shape [9]

Table 2 – Bridge section information [9-10]

| | **Beam height (H/m)** | **Wall thickness (D/mm)** | **Area ($m^2$)** | **Moment of inertia ($m^4$)** |
|---|---|---|---|---|
| **Section 1** | 3 | 450 | 8.5709 | 11.8140 |
| **Section 2** | 2.8 | 360 | 7.7855 | 8.9376 |
| **Section 3** | 2.7 | 360 | 7.7253 | 8.0732 |

Table 3 – Working conditions of the 8 RTHS test cases

| | | | **Working conditions** | | |
|---|---|---|---|---|---|
| **Group** | **Controlling paramter** | **Test cases** | **Velocity (km/h)** | **Smooth road** | **Cross section** |
| 1 | Train velocity | **1** | 200 | Smooth | Cross section 1 |
| | | **2** | 300 | Smooth | Cross section 1 |
| | | **3** | 350 | Smooth | Cross section 1 |
| 2 | Road surface | **4** | 300 | Smooth | Cross section 1 |
| | | **5** | 300 | Not smooth | Cross section 1 |



 



| | | | | | |
|---|---|---|---|---|---|
| 3 | Bridge cross-section stiffness | **6** | 300 | Smooth | Cross section 1 |
| | | **7** | 300 | Smooth | Cross section 2 |
| | | **8** | 300 | Smooth | Cross section 3 |

## 4. Experimental verification

RTHS experimental verification of the proposed ATS+LQG compensation method was conducted for the 8 test cases and its effectiveness is compared to the ATS only method.

### 4.1 Time history response

The commands sent to the shaking table and the displacement responses when using the compensation methods are plotted in Fig. 6 for the first three cases to examine the effect of the different train velocity on the RTHS results.

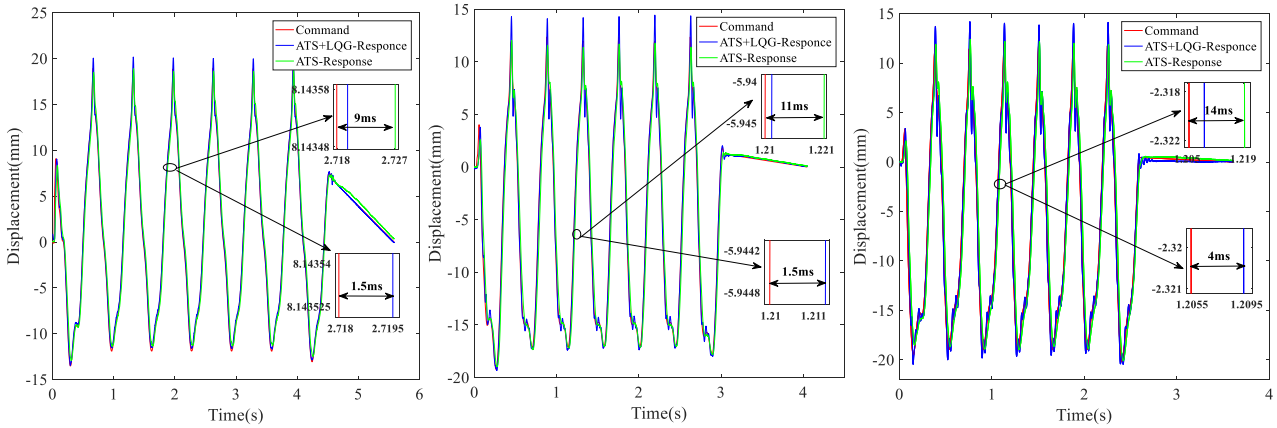


(a) Speed 200km/h (b) Speed 300km/h (c) Speed 350km/h

Fig. 6 – Vehicle-bridge coupling test results at different train speeds

It can be seen that at a speed of 200 km/h, the amplitude of the response signal is very close to the amplitude of the command signal with a time delay of approximately 1.5 ms when using the ATS+LQG method. While the time delay is approximately 9 ms with the ATS only method. When the train speeds are increased to 300 km/h and 350 km/h, the ATS+LQG controller still shows excellent compensation effects, with a time delay of 1.5 ~ 4 ms, as compared to the time delay of 11 ~ 14 ms when using the ATS method. It can also be observed that the time delay increased for both methods when the train speed increases, which can be explained by the fact that there are more high-frequency signals (i.e., f > 15Hz) in the time history responses with the increased train speed.

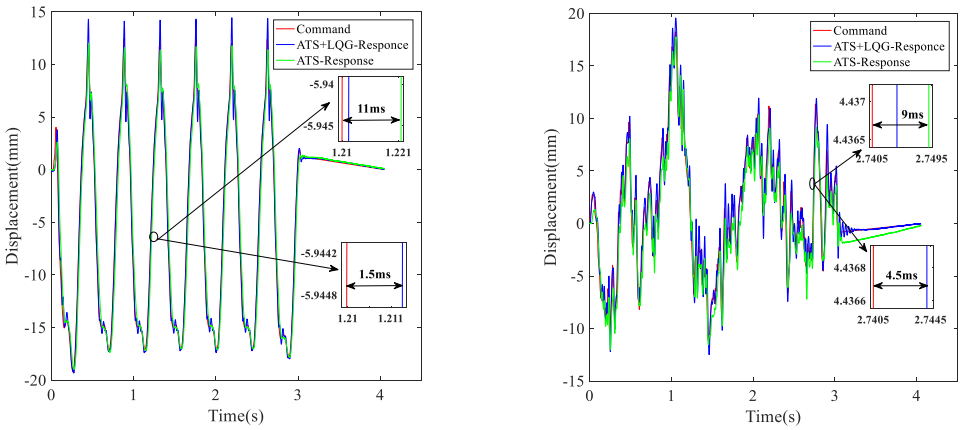


(a) Track smooth (b) Track irregularity



 



Fig. 7 – Test results of track smoothness and irregularity

The responses and commands of cases 4 and 5 are plotted in Fig. 7 to examine the effect of the road surface conditions on the RTHS results. The irregular rail track surface led to much more high frequency signals ranging from 15~50Hz as shown in Fig. 7 (b) when compared to the smooth track surface. Nevertheless, the ATS+LQG method shows better compensation effect with a time delay of about 4.5ms, while the ATS method result in a time delay of 9 ms for the irregular track surface.

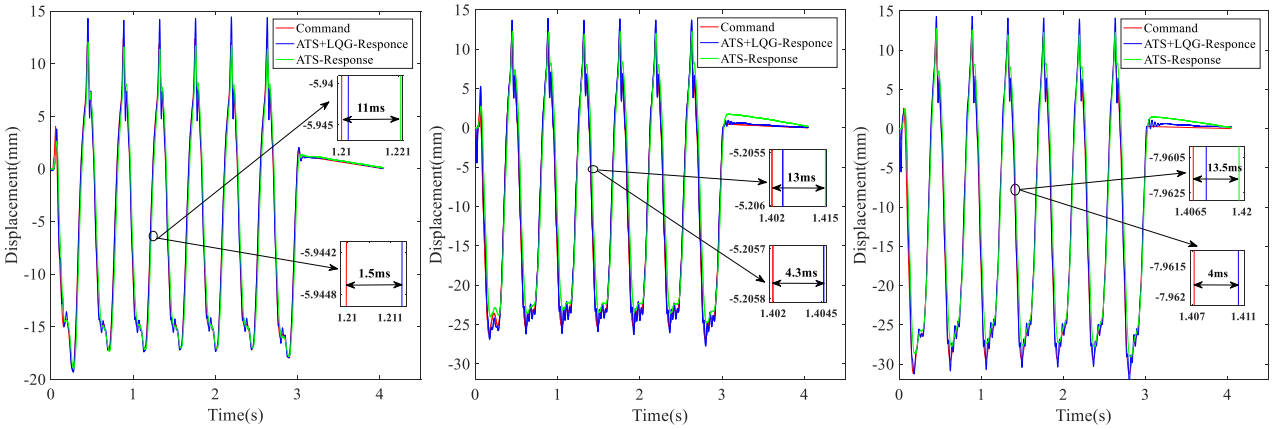


(a) Cross section 1 (b) Cross section 2 (c) Cross section 3

Fig. 8 – Test results at different cross sections

The RTHS results of cases 6~8 are plotted in Fig. 8 to demonstrate the effectiveness of the compensation methods for different bridge cross-section stiffnesses. The delay when using the ATS+LQG method ranges between 1.5 ~ 4 ms for the three bridge cross sections considered herein. While the delay of the ATS method ranges from 11 to 13.5ms. It is demonstrated again that the ATS+LQG method can effectively compensating the delay in the RTHS of the bridge-vehicle coupling system with different bridge cross-section stiffness and it outperformed the ATS method.

## 4.2 Error evaluation

The root-mean-square error (RMSE) between the displacement command and the displacement response of the shaking table is used to further evaluate the compensation methods. The expression of RMSE is:

$$RMSE = \sqrt{\frac{\sum_{i=1}^{N}\left[y_n(i) - x_m(i)\right]^2}{\sum_{i=1}^{N}\left[y_n(i)\right]^2}} \tag{15}$$

where $N$ is the total number of time steps. Table 4 lists the RMSE values of the RTHS results using the ATS+LQG and the ATS compensation methods for the applicable testing cases and summarizes the time delay values observed from the responses shown in Figs. 6~8.

Table 4 – RMSE value and time delay after compensation

| **Testing cases** | **1** | **2** | **3** | **4** | **5** | **6** | **7** | **8** |
|---|---|---|---|---|---|---|---|---|
| **RMSE$_{ATS+LQG}$** | 0.0519 | 0.0701 | 0.0956 | 0.0701 | 0.2511 | 0.0701 | 0.0604 | 0.0673 |
| **Time-delay $_{ATS+LQG}$** | 1.5ms | 1.5ms | 4ms | 2ms | 4ms | 2ms | 4ms | 4ms |
| **RMSE$_{ATS}$** | 0.1283 | 0.1596 | 0.1880 | 0.1596 | 0.2508 | 0.1596 | 0.1421 | 0.1302 |
| **Time-delay$_{ATS}$** | 9ms | 11ms | 14ms | 11ms | 9ms | 11ms | 13ms | 13.5ms |

In general, the time delays in the RTHS using the ATS+LQG compensator (1.5~6 ms) are much smaller than those using the ATS only method (9~14 ms). Similar trend is observed on the RMSE values, which the



 



ATS+LQG method yielded approximately half of the RMSE values of the ATS only method. The smaller RMSE values using the ATS+LQG method demonstrate that the amplitude errors over the entire time history are smaller when using the ATS+LQG method compared to the ATS only method. However, there is one exception of case 5, during which both methods have similar RMSE value that maybe attributed to the very high frequency response (i.e., noisy responses) of the bridge when its surface is irregular.

## 5. Conclusion

To compensate the time delay for high frequency responses expected in the RTHS of the vehicle-bridge coupling system, this paper proposed the combined ATS+LQG compensation method. The ATS+LQG method is verified in the RTHS experiments of 8 working conditions and the following conclusions are drawn:

1) The vehicle-bridge coupling RTHS platform was successfully built to investigate the vehicle-railway bridge interaction of high-speed railway system.
2) For the high-frequency signals expected in RTHS of the vehicle-bridge coupling system, the proposed ATS+LQG controller showed a better compensation effect than the ATS method for different working conditions.

## 6. Acknowledgements

The authors are grateful to Cheng Zeng and Yang Wang of Central South University and Jiliang Wu of Xiamen University for their help with the test. The authors are also grateful to Jianwen Chen, Weixu Song and Qinming Feng of BBK Test Systems Co. Ltd for their work with the pulsar control system. This research is funded by the Scientific Research Fund of the Institute of Engineering Mechanics, China Earthquake Administration (2019C01, 2017A02, 2016A06), and the National Natural Science Foundation of China (51878630, 51378478, 51408565), and the Heilongjiang Provincial Natural Science Fund for Distinguished Young Scholars (JC2018018). Any opinions, findings, conclusions, or recommendations expressed in this paper are those of the authors, and do not necessarily reflect the views of the sponsors.

## 7. References

[1] Watanabe N, Sasaki K (2012): Fundamental tests on a rapid prototype bogie. *Quarterly Report of RTRI*, **53** (4), 199-204.

[2] Nakashima M, Kato H, Takaoka E (1992): Development of real-time pseudodynamic testing. *Earthquake Engng Struct. Dyn*. **21**, 779-792.

[3] Stoten DP, Tu JY, Li G (2009): Synthesis and control of generalized dynamically substructured systems, *Journal of Systems and Control Engineering*, **223** (3),371-392.

[4] Nobuyuki W, Stoten DP (2016): Actuator control for a rapid prototyping railway bogie, using a dynamically substructured systems approach. *Quarterly Report of RTRI*, **57** (2), 90-97.

[5] Wu B, Wang Z, and Bursi OS (2013): Actuator dynamics compensation based on upper bound delay for real-time hybrid simulation. *Earthquake Engineering and Structural Dynamics*, **42** (12), 1749-1765.

[6] Chae Y, Kazemibidokhti K, Ricles JM (2013): Adaptive time series compensator for delay compensation of servo-hydraulic actuator systems for real-time hybrid simulation. *Earthquake Engng Struct. Dyn*, **42** (11), 1697-1715.

[7] Zhou H, Xu D, et al. (2019): A robust linear-quadratic-gaussian controller for the real-time hybrid simulation on a benchmark problem. *Mechanical Engineering and Signal Processing*, **133** (1).

[8] Guo W, Zeng C, et al. (2020): Real-time hybrid simulation for analyzing problem of high-speed train-track-bridge interaction using moving load convolution integral method. in prepare.

[9] Deng Y, Xu S, et al. (2019): Design optimization of simply-supported box beam on high-speed railway. *Railway Standard Design*, **63** (05), 75-79. (In Chinese)

[10] Su Y, Ban X, et al. (2019): Study on optimum design of simply supported box girder on mixed passenger and freight railway. *Railway building*, **59** (01), 6-9. (In Chinese)



 